ELSEVIER

Ceramics International 30 (2004) 1575–1579

CERAMICS INTERNATIONAL

www.elsevier.com/locate/ceramint

Origin of self-aligned nano-domains in MgB_2

S. Li [a,*], T.H. Yip [a], C.Q. Sun [b], S. Widjaja [c], M.H. Liang [a]

[a] *School of Materials Engineering, Nanyang Technological University, Singapore 639798, Singapore*
[b] *School of Electrical and Electronic Engineering, Nanyang Technological University, Singapore 639798, Singapore*
[c] *Corning Incorporated, New York, NY, USA*

Received 26 November 2003; received in revised form 9 December 2003; accepted 22 December 2003

Available online 6 May 2004

Abstract

Random arrangement of B atoms in parent amorphous phase leads to a number of atomic defects, such as dislocations, formed in the reaction product of Mg and B. During the crystallization, dislocation walls form from random arrays of dislocations. Stress at the end of dislocation wall segments attract the surrounding edge dislocations, which are then incorporated and result in wall growth, forming small angle boundaries to connect well-ordered nano-domains. To minimize the energy of the system, the dislocations migrate to interdomain boundaries surrounding the nano-domains. These dislocation rearrangements result in rotation of adjacent nano-domains form a contiguous crystal. By continuing this subgrain rotation process on neighboring nano-domains, large (2 1 1) nano-domains can be aligned as observed by high-resolution transmission electron microscopy (HRTEM). It is demonstrated that the (2 1 1) plane may have the minimum surface energy in MgB_2 and the (2 1 1) zone is the favored orientation for crystal growth.

Keywords: Nano-domains; Crystal growth

1. Introduction

The discovery of superconductivity at 39 K in MgB_2 has initiated enormous scientific interest in order to understand and develop this material to better exploit its high intrinsic performance for magnetic and electronic applications [1,2]. The strongly linked current flow measured from polycrystalline MgB_2 shows that this superconductor class is not compromised by weak-link problem and the supercurrent density in MgB_2 is controlled predominantly by flux pinning rather than by the grain boundary connectivity [3]. In the bulk material, the critical current density (J_c) drops rapidly with increasing magnetic field strength. The magnitude and field dependence of the critical current are related to the presence of structural defects that can "pin" the quantized magnetic vortices that permeate the material. It suggested that the lack of natural defects is responsible for the rapid decline of critical current density (J_c) with increasing field strength [4]. In order to improve the high field performance of MgB_2, a number of techniques, such as proton irradiation, addition of hetero-nanoparticles, fabrication of fine-grained thin films, and oxygen substitution in boron, etc., have been used to induce crystal defects by atomic displacement, inclusions, grain boundaries, and lattice distortion, respectively [5–8]. Recently, a significant flux pinning enhancement in a mixture of MgB_2 and SiC has been reported and an effective vortex pinning source—semi-crystalline defect wells in self-aligned nano-structured MgB_2 was discovered in this material [9,10]. However, the mechanism of the self-aligned nano-structured MgB_2 is still not clear. In this work, we report an investigation in the origin of self-aligned nano-domians in MgB_2.

2. Experimental procedure

MgB_2 samples were prepared by pressing a mixture of Mg 99% purity and amorphous B 99% purity powders in the stoichiometeric ratio of Mg:B = 1:2 with addition of 10 wt.% SiC powder into the pellets. The pellets of dimensions 10 mm × 2 mm were sealed in a Fe tube and subsequently sintered at 700–900 °C for 1 h in flowing high purity Ar atmosphere, followed by furnace cooling to produce MgB_2 (80%) with impurities of MgO (13%) and Mg_2Si (7%) as determined by quantitative X-ray diffraction

* Corresponding author. Fax: +65-6790-4931.
E-mail address: assxli@ntu.edu.sg (S. Li).

0272-8842/$30.00
doi:10.1016/j.ceramint.2003.12.196

(XRD). High-resolution transmission electron microscopy (HRTEM) was conducted on a portion of the as-sintered pellet that was ground under ethanol. Several drops of this suspension was then deposited onto a holey-carbon-coated Cu grid for the HRTEM characterization. Lattice parameters measured and refined by XRD and Rietveld method in the as-sintered MgB_2 sample with the secondary phases (Mg_2Si and MgO) are $a = 3.0856$ Å and $c = 3.5296$ Å, a result within experimental error of original commercial MgB_2 powder ($a = 3.0864$ Å and $c = 3.5227$ Å). It has been reported that the substitution of carbon for boron will cause lattice contraction of a axis from $a = 3.0870$ to 3.0550 Å [11]. Our results indicate that substantial lattice substitution did not occur in the as-sintered sample. This conclusion is also supported by XPS measurement, which shows no shift in Mg^{2+} binding energy in the polyphase material. Element micro-distribution mapped by energy dispersive X-ray spectroscopy shows that the size of MgO and Mg_2Si are in micron scale and are too large to act as vortex pinning centers.

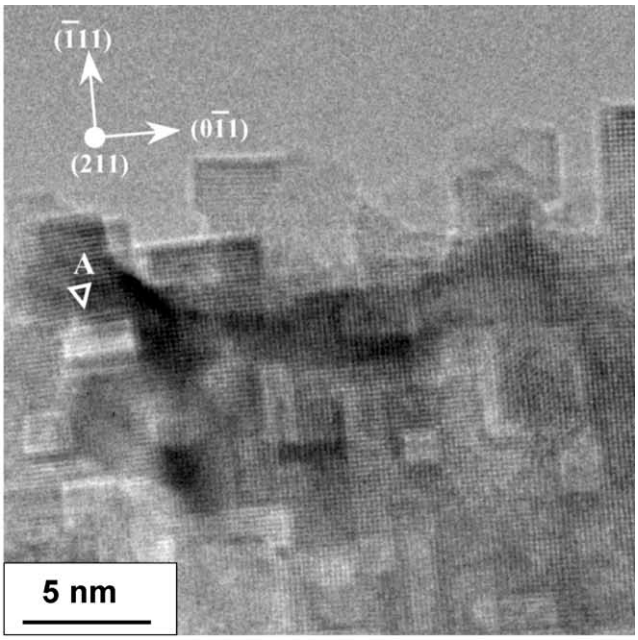

(a)

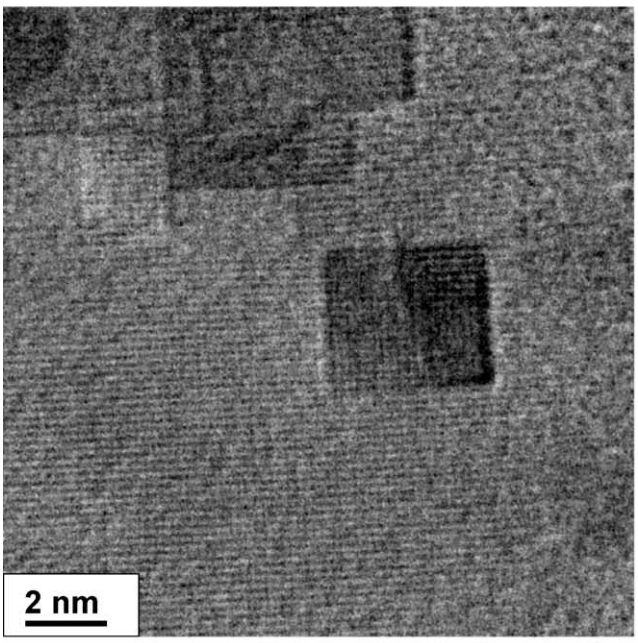

(b)

Fig. 1. (a) HRTEM morphology shows that the majority of the nano-domains with rectangular shapes were aligned along (2 1 1) in self-aligned nano-structured MgB_2. (b) HRTEM morphology shows that a square nano-dot nucleates on (2 1 1) plane.

3. Results and discussion

Fig. 1(a) is an HRTEM lattice image of MgB_2 (2 1 1) planes showing well-aligned nano-domains with rectangular

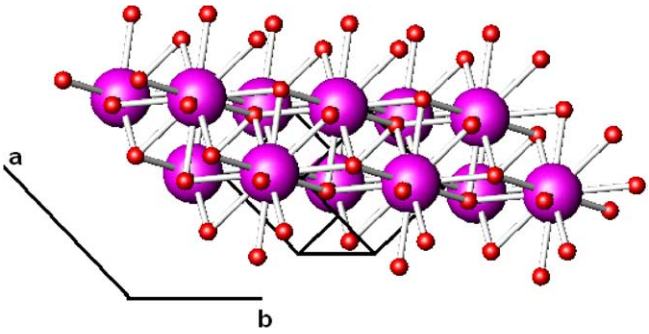

(a)

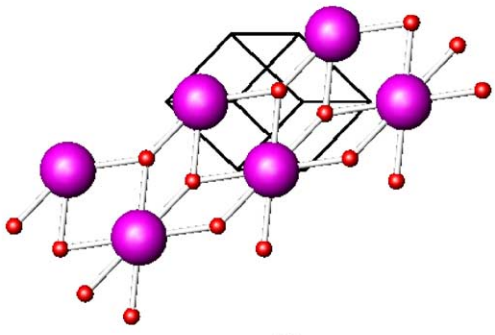

(b)

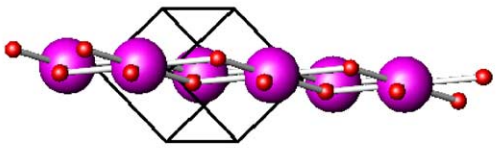

(c)

Fig. 2. A schematic illustration showing an atomic structure of MgB_2 (2 1 1) planes and its crystallographic orientation in unit cell (solid black line): (a) three-dimensional atomic structure, (b) top view, and (c) side view.

shapes of 2–4 nm × 1 nm dimensions. However, alignment is imperfect and a small angle boundary of 2° is discernable in the area marked "A". Such nano-structures were commonly observed in other areas of the sample and it dominates the structure of the material. The morphology at the edge of the observed area in Fig. 1(a) suggests that MgB_2 has nano-scale growth favoring (2 1 1) facetting. The nature of the growth in MgB_2 is also evidenced by the presence of a square island nano-domain, which nucleated and formed on the matrix of (2 1 1) plane, as shown in Fig. 1(b). It is believed that MgB_2 is predisposed to adopt this characteristic geometric form due to favorable surface energy. In the *P*622 crystal structure of MgB_2, 12 B atoms surround each Mg atom in the disposition hexagonal prisms, that are packed together to share (1 0 0) and (0 0 1) faces. Fig. 2 displays the atomic structure of the MgB_2 (2 1 1) plane, showing that each Mg is bonded to six B atoms in the Mg atom plane, note three out-of-plane B above and below the plane. Based on the "broken-bond" model of the surface structure, the surface energy of the MgB_2 (2 1 1) plane should have the minimum surface energy in the system [12]. Although the quantitative surface energy of the (2 1 1) plane is not available, it is believed that the formation energy of stacking faults on (0 0 1) MgB_2 is very large (~945 ergs/nm^2) [13]. It follows that high surface energies are associated with low index planes, including the basal plane.

It has been reported that MgB_2 forms in a process of the diffusion of Mg vapor into an amorphous B matrix [14]. The random arrangement of the B atoms in the amorphous phase leads to a number of atomic defects, such as dislocations, formed in the reaction product of Mg and B. During the crystallization, dislocation walls form from random arrays of dislocations [Fig. 3(a)]. Stress at the end of dislocation wall segments attract the surrounding edge dislocations, which are then incorporated and result in wall growth [Fig. 3(b)], forming small angle boundaries to connect well-ordered nano-domains as shown in Fig. 3(c). To minimize the energy of the system, the dislocations migrate to interdomain boundaries surrounding the nano-domains. These dislocation rearrangements result in rotation of nano-domains A and B to form a contiguous crystal [Fig. 3(d)]. By continuing this subgrain rotation process on neighboring nano-domains [Fig. 3(e)], large (2 1 1) nano-domains can be aligned as observed by HRTEM [Fig. 1(a)].

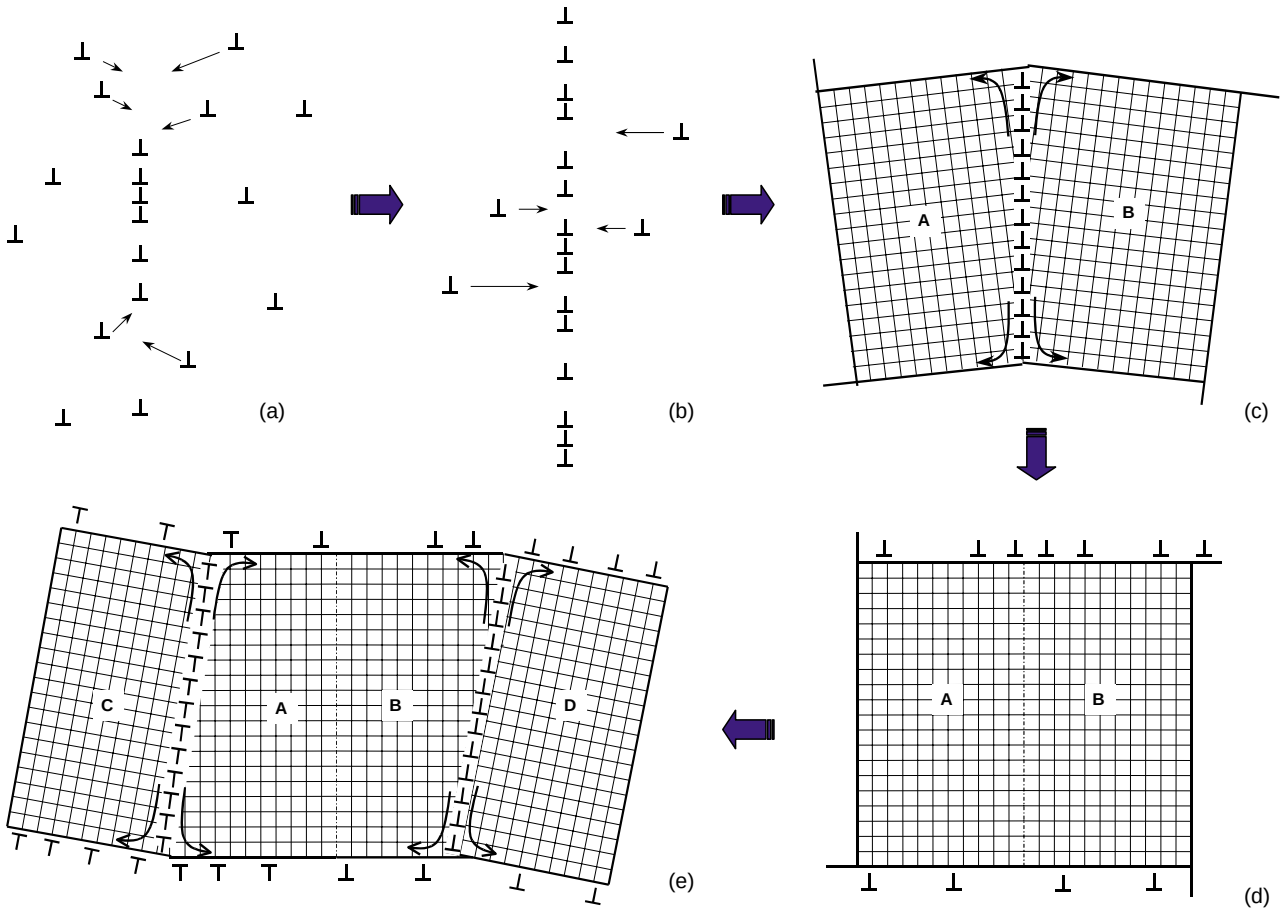

Fig. 3. A schematic illustration showing (a) a random array of dislocations forming in the processing of the diffusion of Mg vapor in the amorphous B matrix, (b) stress at the end of a dislocation wall segment attracting surrounding edge dislocations resulting in wall growth, (c) small angle boundary formation of nano-domains, (d) dislocation rearrangements resulting in a rotation of nano-domains and the dislocation piling in the boundaries after self-alignment, and (e) piled dislocation arrangements from adjacent nano-domains in the horizontal dimension during the self-alignment processing.

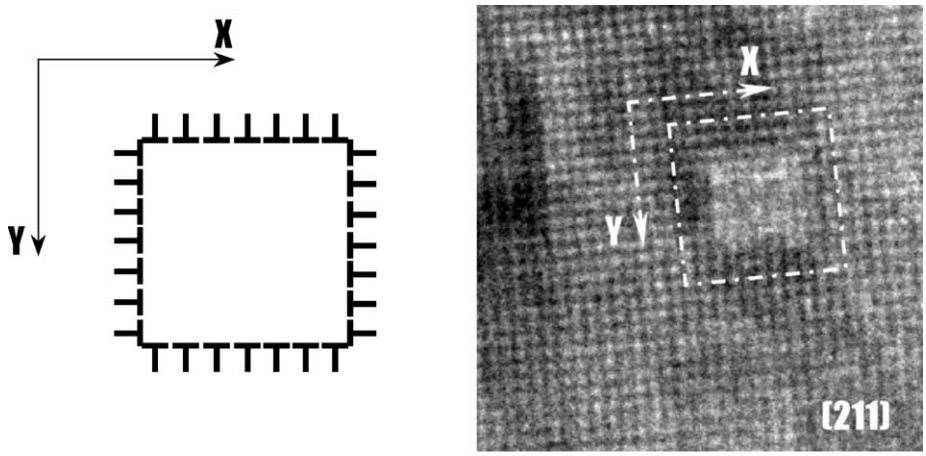

Fig. 4. (a) Schematic of defect well formed through the meeting of dislocations at a point. (b) Nano-defect well observed by HRTEM traps tremendous dislocations to release strain throughout the system, thus facilitating the further alignment of the nano-domains. Note the nano-defect well has semi-crystalline structure, which has been heavily distorted by the trapped numerous dislocations.

The dislocations incorporated into the boundaries can interact with the dislocations incorporated from the neighboring boundaries in two ways: (1) dislocations which have opposite signs from adjacent boundaries would self-compensate and facilitate the further alignment of the nano-domains, and (2) the leading dislocations incorporated from the neighboring boundaries, which have the same sign but opposite slip directions, would restrict each other to slide further, obstructing the dislocation incorporating subsequently and thus inhibiting the alignment. In the latter case, there is a competition between dislocation incorporation and interaction. From the point of thermodynamics, dislocation incorporation from the grain boundaries is the favored process when the number of incorporated dislocations is small. Once the number of dislocations piled in front of the leading dislocation incorporated from the neighboring boundary reaches a threshold level, the alignment of the nano-domains in the area would cease, thus causing higher energy in the surrounding area. This process not only takes place in the horizontal (X) dimension but also the vertical dimension (Y). When the piled dislocations from two dimensions meet at a point with the arrangement as shown in Fig. 4(a), the strain caused by the piled dislocations can be released (although the dislocations with opposite signs in the same dimension cannot offset each other). The dislocation arrangement in Fig. 4(a) results in a defect well to trap the dislocations from the boundaries, further aligning the nano-domains. The HRTEM image in Fig. 4(b) shows a square nano-well (1 nm × 1 nm) surrounded by perfect crystalline nano-domains having identical orientation. The near-atomic resolution detail within the nano-well is consistent with semi-crystalline structure, which was heavily disordered by numerous dislocations and provides direct evidence for the formation of a semi-crystalline defect trap in the self-aligned nano-structured MgB_2. However, defect traps can only release the local strain. To release strain throughout the system, many similar semi-crystalline defect traps are formed and dispersed throughout the material, as shown in Fig. 1(a). It is believed that the addition of SiC in MgB_2 facilitates the formation of self-aligned nano-structured MgB_2 through promotion of incipient melting, but the nature of facilitation is still being studied.

4. Conclusion

The origin of self-aligned nano-domain in MgB_2 has been investigated in detail. Experimental results exhibit that the (2 1 1) plane has the minimum surface energy of the system and the (2 1 1) zone is the favored orientation for crystal growth. Dislocation incorporation from small angle domain boundaries results in further alignment of the nano-domains in three dimensions. On occasions, when orthogonal incorporated dislocations of different signs meet in the (2 1 1) plane at a point, nano-defect wells are formed to release the strain caused by the rotations of nano-domains. This facilitates the further alignment of the nano-domains.

References

[1] J. Nagamatsu, N. Nakagawa, T. Muranaka, Y. Zenitani, J. Akimitsu, Superconductivity at 39 K in magnesium diboride, Nature 410 (2001) 63–64.
[2] D. Larbalestier, A. Gurevich, D.M. Feldmann, A. Polyanskii, High-T_c superconducting materials for electric power applications, Nature 414 (2001) 368–377.
[3] D.C. Larbalestier, L.D. Cooley, M.O. Rickel, A.A. Polyanskil, J. Jiang, S. Patnalk, X.Y. Cai, D.M. Feldmann, A. Gurevich, A.A. Squitieri, M.T. Naus, C.B. Eom, E.E. Hellstrom, R.J. Cava, K.A. Regan, N. Rogado, M.A. Hayward, T. He, J.S. Slusky, K. Khalifah,

K. Inumaru, M. Haas, Strongly linked current flow in polycrystalline forms of the superconductor MgB_2, Nature 410 (2001) 186–189.
[4] Y. Bugoslavsky, G.K. Perkins, X. Qi, L.F. Cohen, A.D. Caplin, Vortex dynamics in superconducting MgB_2 and prospects for applications, Nature 410 (2001) 563–565.
[5] Y. Bugoslavsky, L.F. Cohen, G.K. Perkins, M. Pollchetti, T.J. Tate, R. Gwilliam, A.D. Caplin, Enhancement of the high-magnetic-field critical current density of superconducting MgB_2 by proton irradiation, Nature 411 (2001) 561–563.
[6] C.B. Eom, M.K. Lee, J.H. Chol, L.J. Belenky, X. Song, L.D. Cooley, M.T. Naus, S. Patanik, J. Jiang, M. Rikei, A. Polyanski, A. Gurevich, X.Y. Cai, S.D. Bu, S.E. Babcock, E.E. Hellstrom, D.C. Larbalestier, N. Rogado, K.A. Regan, M.A. Hayward, T. He, J.S. Slusky, K. Inumaru, M.K. Haas, R.J. Cava, High critical current density and enhanced irreversibility field in superconducting MgB_2 thin films, Nature 411 (2001) 558–560.
[7] X.Z. Liao, A.C. Erquis, Y.T. Zhu, J.Y. Huang, D.E. Peterson, F.M. Mueller, H.F. Xu, Controlling flux pinning precipitates during MgB_2 synthesis, Appl. Phys. Lett. 80 (23) (2002) 4398–4400.
[8] J. Wang, Y. Bugoslavsky, A. Berenov, L. Cowey, A.D. Caplin, L.F. Cohen, L.D. Cooley, X. Song, D.C. Larbalestier, High critical current density and improved irreversibility field in bulk MgB_2 made by a scaleable, nanoparticle addition route, Appl. Phys. Lett. 81 (11) (2002) 2026–2028.
[9] S.X. Dou, S. Soltanian, J. Horvat, X.L. Wang, S.H. Zhou, M. Ionescu, H.K. Liu, P. Munroe, M. Tomsic, Enhancement of the critical current density and flux pinning of MgB_2 superconductor by nanoparticle SiC doping, Appl. Phys. Lett. 81 (18) (2002) 3419–3421.
[10] S. Li, T. White, K. Laursen, T.T. Tan, C.Q. Sun, Z.L. Dong, Y. Li, S.H. Zhou, J. Horvat, S.X. Dou, Intense vortex pinning enhanced by semicrystalline defect traps in self-aligned nanostructured MgB_2, Appl. Phys. Lett. 83 (2) (2003) 314–316.
[11] W. Mickelson, J. Cumings, W.Q. Han, Z. Zettl, Effects of carbon doping on superconductivity in magnesium diboride, Phys. Rev. B 65 (2002) 052505–052507.
[12] J.M. Howe, Interface in Materials, Wiley, Inc., New York, 1997, 55 pp.
[13] Y. Yan, M.M. Al-Jassim, Structures, energetics, and effects of stacking faults in MgB_2, Phys. Rev. B 66 (2002) 052502–052505.
[14] P.C. Canfield, D.K. Finnemore, S.L. Bud'ko, J.E. Ostenson, G. Lapertot, C.E. Cunningham, C. Petrovic, Superconductivity in dense MgB_2 wires, Phys. Rev. Lett. 86 (11) (2001) 2423–2426.